W Jacob et al.

Sputtering of iron, chromium and tungsten by energetic deuterium ion bombardment

Sputtering of iron, chromium and tungsten by energetic deuterium ion bombardment

K. Sugiyama, K. Schmid, W Jacob

Max-Planck-Institut für Plasmaphysik, Garching, D-85748 Germany

Abstract

Sputtering of pure materials playing a role in reduced-activation ferritic-martensitic steels, i.e. iron (Fe), chromium (Cr) and tungsten (W) due to energetic deuterium (D) ion bombardment was investigated. Sputtering yields were measured applying thin films in the D bombardment energy range from 60 to 2000 eV/D. The obtained data can be well reproduced by a semi-empirical formula suggested by Bohdansky, and the corresponding fitting parameters are provided. It is confirmed that analytical formulae suggested by Eckstein and Yamamura agree satisfactorily with experimental data. By comparison with results from the binary-collision-approximation-based calculation codes SDTrimSP and SRIM it is found that SRIM has some limitations in simulating sputter yield close to the threshold whereas SDTrimSP results showed good agreement with measured data in the investigated energy range.

1. Introduction

Sputtering of plasma-facing-wall materials due to interaction with energetic ions (particularly hydrogen isotopes) is an essential issue in magnetically confined fusion devices because it is directly related to impurity generation as well as to the lifetime of plasma-facing components [1]. Sputtering behavior of candidate materials, such as beryllium and carbon, due to energetic hydrogen isotope ion bombardment was extensively studied in the last several decades [2]. Reduced-activation ferritic-martensitic (RAFM) steels, such as EUROFER [3], RUSFER [4], the Japanese alternative F82H [5] or the Chinese CLAM [6] which are being developed as structural materials for fusion applications, are recently also considered as a possible option for certain areas of plasma-facing surfaces in a future power plant because of technological and economic advantages [7]. In this sense, evaluation of EUROFER steel erosion by energetic deuterium (D) bombardment has started recently [8]. Sputtering of RAFM steel is not as simple as that of pure materials because steel is a compound material. For example, one can theoretically expect that lighter alloyed elements will be preferentially sputtered, leading to a continuous change of the surface stoichiometry during ion irradiation. For a better understanding/prediction of the sputtering processes on RAFM steels it is in a first step necessary to know the sputtering of each alloyed element as a reference. However, sputtering data for these elements are still quite limited.

In this study, therefore, we measure the sputtering yields of some of key elements for RAFM steels, i.e. iron (Fe: the base material), chromium (Cr: the second major alloyed element ($\sim$ 10 at.%)) and tungsten (W: the highest-Z admixed element in RAFM steels), under well-defined conditions in order to obtain comprehensive data sets for these constituents. The obtained data are further evaluated with fitting formulae for a parametrization and analytic description of the measured sputtering yields. Furthermore, the experimental data are compared with existing sputtering simulation codes for benchmarking. This step is essential because the erosion rate of steel walls in future fusion devices will be eventually assessed numerically by using such simulation codes.

2. Experimental procedure

2.1. Sample preparation

Thin layers of Fe, Cr and W were prepared by magnetron-sputter deposition using UNIVEX 450B device (Leybold Vacuum GmbH). Single-crystalline silicon (Si) wafers were used as substrates. The sample dimension was 12 mm $\times$ 15 mm, being defined by the sample holder of the ion irradiation setup. In order to ensure the layer adhesion the Si substrate surface was cleaned by argon (Ar) RF plasma etching for 1 min. prior to the layer deposition. Ar was also used as working gas during deposition with the pressure of 0.3 Pa, while the background pressure inside the deposition chamber is $\sim$ 2-3$\times$10^{-5} Pa. High power DC-discharge was applied for the magnetron-sputtering of the target (600 W for Fe and Cr, and 300 W for W deposition). The deposition rate was roughly 20 nm/min and the

thickness of the deposited layers was 350 - 400 nm. No bias voltage was applied to the substrate holder. Under this deposition condition the Ar content in the deposited layers is below the detection limit of the applied ion-beam analysis (see below). In each deposition run a graphite substrate was installed together with the Si substrates. This allows the measurement of low-Z impurities, such as oxygen (O), in the layers by ion-beam analysis. The determined O concentrations in the layers were about 2-3 at.% for Fe and W and about 5-6 at.% for Cr.

2.2. Deuterium ion irradiation

Prepared specimens were then irradiated by D ions in the high-current ion source set-up (HSQ) at IPP Garching [9]. The HSQ set-up consists of a duo-PIGatron type ion source [10], some differential pumps at different stages, a magnetic analyzer for beam deflection and a target irradiation chamber connected with a load-lock sub-chamber, as schematically shown in figure 1. The magnetic analyzer enables to provide a mass-separated D ion beam at defined ion energy, which is well suited for fundamental sputtering yield measurements. The D energy can be controlled by the ion acceleration voltage and the sample biasing. Since the dominant ion component generated in the ion source is D_3^+, D_3^+ ions were chosen as the bombarding species to achieve higher ion beam currents. These molecular D_3^+ ions are considered to be identical to 3 individual D ions impinging with the same velocity as the molecular ion. Correspondingly, the energy per deuteron is 1/3 of the experimentally applied ion energy and the flux is three times the measured ion flux. In this study, the sputtering yield was measured in the D energy range from 60 to 2000 eV/D. The ion beam incident angle was normal to the sample surface. The ion bombardment induces some change of the surface morphology resulting in the appearance of visible "footprint" of the D ion beam. The ion beam spot area was determined by measuring the footprint size. It varies from 0.3 to 0.85 cm^2 depending on the D energy. The experimental ion fluxes and fluences were calculated from the measured ion currents and beam spot areas. This includes the implicit assumption that the beam intensity is relatively homogeneous across the beam spot. In fact the variation of irradiation beam intensity was checked by measuring the lateral erosion profile after the D irradiation by scanning the ion-beam analysis beam spot over the sample. The ion-beam analysis beam spot size is about 1 mm^2 and, therefore, significantly smaller than the D irradiation beam spot. The such-determined variation of the current density over the beam spot is of the order of 10 to 20 %. The beam spot area was measured as precisely as possible, nevertheless, the determined area size is expected to include 10 – 20 % of measurement error. This uncertainty of the beam flux affects the determination of the local beam flux and fluences and the evaluation of the RBS data (see below) but not the evaluation of the weight loss measurements. The ion beam current at the target is typically $\sim 10^{-5}$ A, corresponding to a deuteron flux of $\sim 10^{19}$ Dm^{-2}s^{-1}. The irradiation fluences in this work were varied in the range of 1-3$\times$10^{23} Dm^{-2} corresponding to exposure durations between 3 and 9 h. Since the background pressure in the target irradiation chamber is sufficiently low ($\sim 10^{-6}$ Pa), surface oxidation during irradiation is not expected. The sample was not actively cooled during

irradiation, resulting in slight temperature rise to 310 up to 360 K depending on the ion impinging energy.

2.3. Post-irradiation analyses

The sputtering yield was evaluated by weight-loss (WL) technique and Rutherford Backscattering Spectrometry (RBS). For WL, the sample weight was measured ex-situ before and after D irradiation by a microbalance system (Sartorius MC21S) having a weight resolution of 1 μg and the measurement uncertainty of ± 3 μg. The sputtering yield was then calculated from the weight loss and the total number of D atoms. The measurement error for WL was estimated from the above mentioned measurement uncertainty. For D irradiation energies near the threshold energy, higher D fluences were accumulated to achieve sufficient weight changes. Nevertheless, the weight loss was in these cases relatively small (around 10 μg), resulting in a larger relative error. On the other hand, the relative error becomes smaller in the higher energy range where sufficient weight losses were usually obtained (up to ~ 50 μg).

RBS measurements were performed using 3.0 MeV ^{4}He ions as probe beam. The ^{4}He$^+$ beam was provided by a 3 MV Tandem accelerator connected to an ion beam analysis chamber. A beam aperture in front of the sample limits the ^{4}He$^+$ irradiation spot size to 1 mm × 1 mm at the sample surface, meaning that the ^{4}He$^+$ beam size is sufficiently smaller than the D ion irradiation spot area. The RBS measurements were performed in the center of the D ion irradiation spot. The backscattered ^{4}He$^+$ was analyzed by a solid detector located at the laboratory angle of 165°. Figure 2 shows examples of RBS spectra obtained from a Fe layer before and after D ion irradiation using different irradiation conditions. Backscattering from the thin Fe layer gives rise to the rectangular-shaped peak in the backscatter-energy range of about 1950 to 2300 keV. The highest backscatter energy (about 2300 keV) is from backscattering at the Fe surface and the thickness of the Fe layer is characterized by the width of this peak. Backscattering from the silicon substrate produces the step visible at lower energy. Because projectile ions reaching the interface have to travel through the Fe layer at the sample surface they experience an energy loss depending on the thickness of the Fe layer. As a result, the position of the Si step depends on the thickness of the Fe layer and changes in close correspondence to the width of the Fe peak. As can be seen in figure 2, the layer thickness of the Fe layer changes by D irradiation depending on the D ion energy and fluence. Each RBS spectrum was evaluated with the SIMNRA program [11] to quantitatively determine the thickness change. The sputtering yield was then determined by the thickness change and the D ion fluence. The RBS setup used in this study is well calibrated and the experimental uncertainty is expected to be ~ 10 %. In practice it is difficult to determine thickness changes of less than 10^{16} at./cm^2. Therefore, this value is taken as the minimum absolute uncertainty for RBS. Consequently, for cases where the thickness change is small the absolute uncertainty becomes comparable with this detection limit and the relative uncertainty becomes large. As mentioned above, the D fluence was determined by measuring the total

accumulated D ion charge and the ion irradiation beam spot area size assuming a homogeneous ion flux across the beam spot area. The uncertainty of the determination of the irradiation beam spot area (see above) was taken into account in the evaluation of the RBS data. The total uncertainty associated with the RBS data evaluation was finally estimated using common error propagation taking those technical uncertainties of the RBS and the ion fluence calculation into account.

3. Results and discussion

3.1. Experimental results and the yield curve fitting

Figure 3 shows sputtering yield data of each element as a function of the D bombardment energy. Additionally, the data are summarized in table 1. The sputtering yields measured by weight loss (WL) and by RBS agree within the experimental uncertainties. However, at the higher ion energies (> 5 times the threshold energy) there seems to be a systematic small deviation between both methods. The RBS-measured yields are slightly higher than the WL yields. This can be explained by the additional uncertainties in the RBS evaluation due to the possible peaking of the beam profile and the determination of the precise beam area as discussed in Sect. 2.3. Because the RBS data are measured in the center of the irradiation beam spot a peaking would lead to a higher local fluence than the calculated mean fluence. In the evaluation this would lead to slightly higher yield. For the evaluation of the WL data this effect does not occur. On the other hand, the RBS measurements are advantageous at low energies where the yields are low. In this region the evaluation of the WL data suffers from a relatively large uncertainty.

Available literature data for Fe and W [9] are also shown in the figure. The present data are comparable with the published data within the experimental uncertainty, but they are systematically higher (for W up to a factor of 2). The reason for that is not clear. One difference is that the previous studies were performed using polycrystalline bulk samples, whereas sputter-deposited thin layers were used in this study. Although we do not anticipate that this influences sputtering, we cannot exclude it. Another possible explanation is the difference of impurity content (e.g. O) between the bulk samples and the deposited layers. Our layers have a small oxygen content of a few at.% (see Sect. 2.1).

The experimental data were fitted with the well-known empirical Bohdansky formula [12], which was developed based on the analytical sputtering theory by Sigmund [13]. Accordingly, the sputter yield Y is given as:

$$Y(E) = QS_n(\varepsilon)\left(1 - \left(\frac{E_{th}}{E}\right)^{\frac{2}{3}}\right)\left(1 - \frac{E_{th}}{E}\right)^2$$

where Q is the yield pre-factor, $S_n(\varepsilon)$ is the nuclear stopping cross section, E is the projectile energy and E_{th} is the threshold energy of the sputtering. For this fitting, $S_n(\varepsilon)$ was calculated with using the Kr-C interaction potential model [14], i.e.,

$$S_n(\varepsilon) = \frac{0.5\ln(1 + 1.2288\varepsilon)}{\varepsilon + 0.1728\sqrt{\varepsilon} + 0.008\varepsilon^{0.1504}}$$

with the reduced energy ε of

$$\varepsilon = E \frac{M_2}{M_1 + M_2} \frac{a_L}{Z_1 Z_2 e^2}$$

as proposed by García-Rosales *et al*. [15]. M_1 and M_2 are the masses and Z_1 and Z_2 are the atomic numbers of the projectile and the target atoms, respectively. e is the electron charge and α_L is the Lindhard screening length given as

$$a_L = \left(\frac{9\pi^2}{128}\right)^{\frac{1}{3}} a_B \left(Z_1^{2/3} + Z_2^{2/3}\right)^{-\frac{1}{2}}$$

where α_B is the Bohr radius. In many cases Q and E_{th} are used as free fitting parameters. However, in this work, E_{th} was not taken as a free parameter but determined by

$$E_{th} = \frac{E_{sb}}{\gamma(1 - \gamma)},$$

with

$$\gamma = \frac{4M_1 M_2}{(M_1 + M_2)^2}.$$

E_{sb} is the surface binding energy of the target material. In general it is taken equal to the heat of sublimation, which is a known value, and here, the E_{sb} values are taken from Ref. [9]. In this work, accordingly, the pre-factor Q was only the free parameter to fit the experimental data. It is sometimes argued that the empirical Bohdansky formula is not always perfect to reproduce the experimental result over a large energy range. However, the fitting is very reasonable for all three elements investigated here (see figure 3). Values of E_b, and E_{th} used in this study, and Q obtained by this fitting procedure are summarized in table 2.

3.2. Comparison with other analytical formulae

Other analytical descriptions of sputtering yields which are widely accepted in the community today are semi-empirical formulae proposed by Eckstein *et al*. [16-18] and Yamamura *et al*. [19] (see Appendix). Eckstein's formula is based on the Bohdansky formula, but revised to improve the yield description, particularly, near the threshold energy. The Yamamura formula is based on Sigmund's sputtering theory as well as on the Bohdansky formula. The first Yamamura formula was better suited to reproduce sputtering for cases of heavy-ion projectiles [20]. It was later modified to extend it to the

cases of light-ion projectiles where the particle reflection plays an important role for the sputtering [19,21]. In general, a drawback in using these formulae for evaluation of experimental data is that there are multiple free parameters for the fitting. It is not simple to determine the parameter combinations unambiguously. For this the reason the empirical Bohdansky formula is applied for fitting the sputtering yield in this study. Nevertheless, both Eckstein and Yamamura have provided parameter combinations for a large number of projectile-target cases by fitting their formulae to theoretical results determined using their own simulation codes based on the binary collision approximation (BCA), i.e., TRIM.SP [22] and ACAT [23], respectively. In figure 3, yield curves from those analytical formulae with given fitting parameters (see Appendix) are shown as well. In general, both formulae show similar sputtering yields and reproduce the experimental data acceptably. Particularly, the Eckstein curve fits almost perfectly to this experimental data near the threshold energy.

3.3. Comparison with BCA-based calculation codes

As mentioned, benchmarking and validation of BCA-based calculation codes is one of the major objectives of this study. In this respect, the present experimental data are additionally compared with results from the calculation codes SDTrimSP [24] and SRIM [25].

SDTrimSP code is based on the static Monte-Carlo simulation code TRIM.SP [22] and its dynamic version TRIDYN [26]. The latter allows dynamic simulations taking stoichiometry changes as a function of fluence into account. In this study, the sputtering calculation was performed with SDTrimSP version 5.00 [27]. The program provides a number of input parameters and allows selecting several options for performing the simulations. For calculation of the sputtering yield the decisive parameters are the surface binding energy and the interaction potential. The surface binding energy for each target material used in this study were the known heats of sublimation, i.e., the same values as listed in table 2, and the Kr-C potential (default in SDTrimSP) was chosen as interaction potential. Other important calculation options were also set to default, e.g., the MAGIC method [28] was used for calculation of the scattering integral, and the inelastic stopping power was treated by equipartition of Lindhard-Scharff [29] and Oen-Robinson [30] models.

SRIM [25] is probably the most widely distributed calculation program used for various purposes, such as ion range, damage cascade profile and sputtering simulations. In this study, the sputtering was calculated using "Calculation of Surface Sputtering" option in SRIM-2013 package. Surface binding energy is also an input variable in SRIM, but the heat of sublimation is set as the default value. For the calculation presented here the surface binding energies used in SRIM were identical to those used in the SDTrimSP calculations.

Figure 4 shows the comparison between code calculation results and the present experimental data. The SDTrimSP outputs for Fe and Cr show yields close to the experimental results, agreeing within ± 20 % in most of the measured energy range. For W, the SDTrimSP results are somewhat higher than

the experimental data. Nevertheless, the difference is still within ~ 50 % in the measured energy range. Overall, one can conclude that SDTrimSP results are in reasonable agreement with the experimental results for all three investigated elements. On the other hand, SRIM simulation results disagree in some cases substantially from the experimental data. Although the results for Fe and Cr agree reasonably with the experimental results for energies above ~ 300 eV/D, in both cases the yields deviate significantly in the lower energy range close to the threshold energy. Namely, the drop of the sputtering yield occurs at much higher energies than in the experimental data and in the SDTrimSP results. The SRIM result for W also shows the similar deviation around the threshold energy. Furthermore, in the case of W, it shows a relatively large difference also in the energy range above 500 eV/D, i.e., the W sputtering yield calculated by SRIM is always higher than the experimental results by more than factor of 2. The strong deviation of the SRIM results found near the threshold energy can lead to a severe underestimation of the real sputtering yield in that energy range. As mentioned above, one could vary the surface binding energy for the SRIM sputtering calculation trying to improve the agreement, but the simulations with reduced surface binding energies did not lead to a notable improvement for all three investigated elements. Another possible explanation for the differences between SRIM and SDTrimSP could be the chosen interaction potential in the simulations. In SRIM, the inter-atomic interaction and inelastic stopping power are approximated using the Ziegler-Biersack-Littmark (ZBL) universal potential model [25]. Hofsäss *et al*. recently pointed out that it seems that the ZBL potential has some limitations to describe low energy binary collisions [31]. Since SDTrimSP allows choosing different interaction potentials, we tested the influence of the used potential model within SDTrimSP by comparing results for the ZBL potential with those for the Kr-C potential. Compared to the Kr-C potential, the simulation with the ZBL potential provides worse agreement with the experimental results. Sputtering yields calculated for Fe and W using the ZBL potential were systematically higher by a factor of ~1.4 compared with the yields calculated with the Kr-C potential which are already up to 50 % higher than the current experimental data. Nevertheless, in SDTrimSP, the ZBL potential gives still finite yield values in the energy range around the threshold in contrast to SRIM which showed 0 yield in that energy range. This means that the used potential model can somewhat influence the sputtering simulation, however, it is not the reason explaining the observed difference between SRIM and SDTrimSP in the energy range at and slightly above the threshold. This comparison indicates that SRIM has some other intrinsic deficiencies for calculating sputtering yields near the threshold energy.

4. Summary

Sputtering yields of RAFM-related materials: Fe, Cr and W by energetic D ion bombardment were measured by means of the thin film technique under well-defined laboratory conditions. The

bombardment energy range was from 60 to 2000 eV/D, which is relevant for the ion-material interaction in fusion devices.

The measured data were evaluated with a conventional semi-empirical fit formula suggested by Bohdansky *et al.* [12]. Experimental results are well fitted by the Bohdansky formula. Furthermore, it was confirmed that analytical formulae suggested by Eckstein *et al.* and Yamamura *et al.* with given fitting parameters (see Appendix) also agreed acceptably with the experimental data.

Comparison with BCA-based calculation codes shows that SDTrimSP provides a reasonable description of the sputter yields as a function of ion energy whereas SRIM calculation results shows a significant underestimation near the threshold energy. This indicates that SRIM has some limitations to describe the low energy binary collision, and accordingly, SDTrimSP is better suited to simulate sputtering yields in the fusion-relevant energy range.

Appendix

In Eckstein's formula [16-18], the sputtering yield $Y(E)$ is given as

$$Y(E) = QS_n(\varepsilon) \frac{\left(\frac{E}{E_{th}} - 1\right)^{\mu}}{\frac{\lambda}{\omega(\varepsilon)} + \left(\frac{E}{E_{th}} - 1\right)^{\mu}}.$$

The pre-factor: Q and the nuclear stopping cross-section: $S_n(\varepsilon)$ are the same as in the Bohdansky formula, while the term dealing with the threshold is modified and two additional fitting parameters: λ and μ are introduced. $\omega(\varepsilon)$ is given as

$$\omega(\varepsilon) = \varepsilon + 0.1728\sqrt{\varepsilon} + 0.008\varepsilon^{0.1504}$$

with the reduced energy: ε as defined in the body of the text.

The Yamamura [19] formula is given as

$$Y(E) = 0.042Q \frac{\alpha(M_2/M_1)}{E_{sb}} \frac{S_n(\varepsilon)}{1 + \Gamma S_e \varepsilon^{0.3}} \left(1 - \sqrt{\frac{E_{th}}{E}}\right)^s$$

where

$$\alpha\left(\frac{M_2}{M_1}\right) = 0.249\left(\frac{M_2}{M_1}\right)^{0.56} + 0.0035\left(\frac{M_2}{M_1}\right)^{1.5}$$

and the term Γ is

$$\Gamma = \frac{W}{1 + \left(\frac{M_1}{7}\right)^3}.$$

The nuclear stopping cross section: $S_n(\varepsilon)$ used in Yamamura formula is a modified Thomas-Fermi approximation given as

$$S_n(\varepsilon) = 8.478 \frac{Z_1 Z_2}{\sqrt{Z_1^{\frac{2}{3}} + Z_2^{\frac{2}{3}}}} \frac{M_1}{M_1 + M_2} \frac{3.441\sqrt{\varepsilon}\ln(\varepsilon + 2.718)}{1 + 6.355\sqrt{\varepsilon} + \varepsilon(6.882\sqrt{\varepsilon} - 1.708)},$$

with the reduced energy: ε, as defined in the body of the text. S_e is the Lindhard inelastic stopping coefficient given as

$$S_e = \left(\frac{9\pi^2}{128}\right)^{\frac{1}{3}} \frac{(M_1 + M_2)^{\frac{3}{2}}}{M_1^{\frac{3}{2}} M_2^{\frac{1}{2}}} \frac{Z_1^{\frac{3}{2}} Z_2^{\frac{1}{2}}}{\left(Z_1^{\frac{1}{3}} + Z_2^{\frac{2}{3}}\right)^{\frac{3}{4}}}.$$

Accordingly, Q, W and s are parameters for fitting.

As mentioned in the body of the text, both authors have given the fitting parameters for each projectile-target combination in Refs. [18,19], as listed in table 3.

References

[1] G. Federici et al., Nuclear Fusion **41** (2001) 1967-2137

[2] C. H. Skinner et al., Fus. Sci. Eng. Technol. **54** (2008) 891-945.

[3] B. van der Schaaf, F. Tavassoli, C. Fazio et al., Fusion Eng. Des. **69** (2003) 197

[4] V.M. Chernov, M.V. Leonteva-Smirnova, M.M. Potapenko, et al., Nucl. Fusion 47 (2007) 839-848.

[5] S. Jitsukawa, M. Tamura, B. van der Schaaf, et al., J. Nucl. Mater. 307-311 (2002) 179-186.

[6] Q. Huang, FDS Team, J. Nucl. Mater. 455 (2014) 649-654.

[7] D. Maisonnier, I. Cook, S. Pierre et al., Fusion Eng. Des. **75-79** (2005) 1173

[8] J. Roth, K. Sugiyama, V. Alimov et al., J. Nucl. Mater. **454** (2015) 1

[9] W. Eckstein, C. García-Rosales, J. Roth, W. Ottenberger, "Sputtering Data", IPP Report 9/82 (1993), Max-Planck-Institut für Plasmaphysik, Garching, (http://hdl.handle.net/11858/00-001M-0000-0027-6324-6)

[10] R.C. Davis, T.C. Jemigan, O.B. Morgan et al., Rev. Sci. Instrum. **46** (1975) 576

[11] M. Mayer, "SIMNRA User's Guide", IPP Report 9/113 (1997) Max-Planck-Institut für Plasmaphysik, Garching, (http://hdl.handle.net/11858/00-001M-0000-0027-6157-F)

[12] J. Bohdansky, Nucl. Instr. and Meth. B **2** (1984) 587

[13] P. Sigmund, Phys. Rev. **184** (1969) 383

[14] W.D. Wilson, L.G. Haggmark and J.P. Biersack, Phys. Rev. B **15** (1977) 2458

[15] C. García-Rosales, W. Eckstein, J. Roth, J. Nucl. Mater. **218** (1994) 8-17

[16] W. Eckstein, R.Preuss, J. Nucl. Mater. **320** (2003) 209

[17] W. Eckstein, Vacuum **82** (2008) 930

[18] R. Behrisch, W. Eckstein, "Sputtering by Particle Bombardment, Experiments and Computer Calculations from Threshold to MeV Energies" Topics in Applied Physics, vol.110, Springer (2007)

[19] Y. Yamamura, H. Tawara, Atom Data Nucl. Data Tables **62** (1996) 149

[20] Y. Yamamura, Radiat. Eff. **55** (1981) 49

[21] Y. Yamamura, N. Matsunami, N. Itoh, Radiat. Eff. **71** (1983) 49

[22] J.P. Biersack, W. Eckstein, Appl. Phys. A **34** (1984) 2

[23] Y. Yamamura, Y. Mizuno, IPPJ-AM-40, Nagoya University (1985)

[24] W. Eckstein, R. Dohmen, A. Mutzke et al., "SDTrimSP: A Monte-Carlo code for calculating collision phenomena in randomized targets", IPP Report 12/3 (2007), Max-Planck-Institut für Plasmaphysik, Garching, (http://hdl.handle.net/ 11858/00-001M-0000-0027-04E8-F)

[25] J.F. Ziegler, J.P. Biersack, M.D. Ziegler, "SRIM – The stopping and ranges of ions in matter", SRIM Co. (2008), http://www.srim.org/

[26] W. Möller, W. Eckstein, J.P. Biersack, Comput. Phys. Commun. **51** (1988) 355

[27] A. Mutzke, R. Schneider, W. Eckstein. and R. Dohmen, "SDTrimSP version 5.00", IPP Report **12/08** (2011), Max-Planck-Institut für Plasmaphysik , Garching, (http://hdl.handle. net/11858/00-001M-0000-0026-EAF9-A)

[28] J.P. Biersack, L.G. Haggmark, Nucl. Instr. and Meth. **174** (1980) 257

[29] J. Lindhard and M. Scharff, Phys, Rev. **124** (1961) 128

[30] O.S. Oen and M.T. Robinson, Nucl. Instr. and Meth. **132** (1976) 647

[31] H. Hofsäss, K. Zhang, A. Mutzke, Applied Surface Science **310** (2014) 134

Table 1.

Sputtering yield data of Fe, Cr and W experimentally determined in this study. "WL" stands for the data determined by weight-loss measurement whereas "RBS" is by Rutherford Backscattering spectrometry. The value in a round bracket shown next to each yield value is the estimated absolute error.

D energy [keV]	Fe				Cr				W			
	WL	(error)	RBS	(error)	WL	(error)	RBS	(error)	WL	(error)	RBS	(error)
0.06	2.30E-3	(1.9E-3)	9.4E-4	(2.3E-4)	2.92E-3	(2.0E-3)	1.08E-3	(2.6E-4)				
0.1	7.69E-3	(3.6E-3)	0.0101	(2.3E-3)	6.46E-3	(3.9E-3)	9.56E-3	(2.2E-3)				
0.2	0.0292	(4.3E-3)	0.0226	(5.1E-3)	0.0435	(4.8E-3)	0.0297	(6.7E-3)				
0.3	0.0255	(5.4E-3)	0.0336	(7.5E-3)	0.0546	(5.1E-3)	0.0373	(8.4E-3)			3.0E-4	(2.5E-4)
0.4	0.0394	(6.4E-3)	0.0412	(9.2E-3)							1.17E-3	(5.5E-4)
0.5	0.0407	(5.0E-3)	0.0563	(1.3E-2)	0.0422	(5.7E-3)	0.0549	(1.2E-2)	1.14E-3	(6.8E-4)	1.41E-3	(6.4E-4)
0.7	0.0463	(4.7E-3)	0.0571	(1.3E-2)	0.0381	(5.9E-3)	0.0626	(1.4E-2)	1.62E-3	(6.2E-4)	3.11E-3	(1.1E-3)
1.0	0.0413	(4.5E-3)	0.0740	(1.7E-2)	0.0466	(5.9E-3)	0.0680	(1.5E-2)	6.12E-3	(1.2E-3)	6.30E-3	(2.1E-3)
1.5	0.0347	(1.0E-2)	0.0542	(1.2E-2)	0.0538	(8.4E-3)	0.0689	(1.5E-2)	6.29E-3	(1.1E-3)	7.84E-3	(1.8E-3)
2.0	0.0312	(1.0E-2)	0.0400	(9.0E-3)	0.0489	(7.9E-3)	0.0584	(1.3E-2)	5.36E-3	(1.0E-3)	9.58E-3	(2.2E-3)

Table 2

Summary of surface binding energy: E_{sb}, sputtering threshold energy for D ion bombardment: E_{th} used in the fitting procedure, and the obtained pre-factor Q for each target element.

	Surface binding energy: E_{sb} [eV]	Threshold energy: E_{th} [eV]	Fitting factor: Q
Cr	4.12	33.7	0.179
Fe	4.34	37.5	0.154
W	8.68	216	0.034

Table 3

Fitting parameters for Eckstein [18] and Yamamura [19] formulae. Parameters are all given by each author.

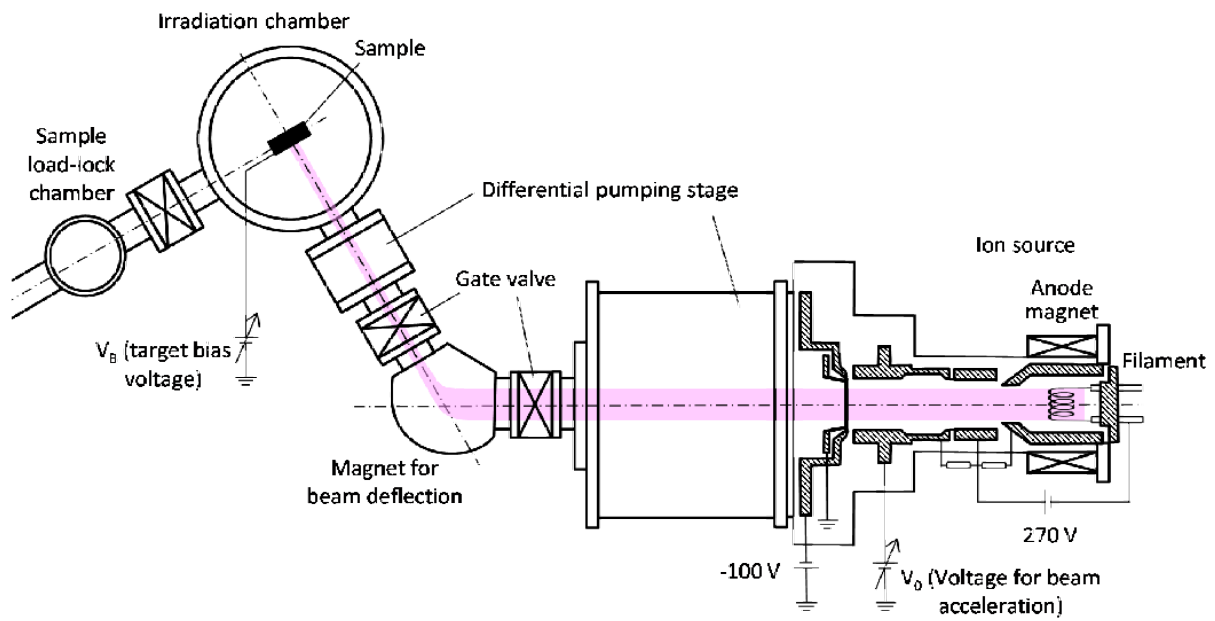|	Eckstein formula [18]				Yamamura formula [19]			
	Q	E_{th} [eV]	λ	μ	Q	E_{th} [eV]	W	s
Cr	0.1084	35.0	0.2899	1.7152	0.93	35.0	1.44	2.5
Fe	0.0919	40.9	0.2743	1.3489	0.75	38.6	1.2	2.5
W	0.0183	228.8	0.3583	1.441	0.72	222.0	2.14	2.8

Figure 1

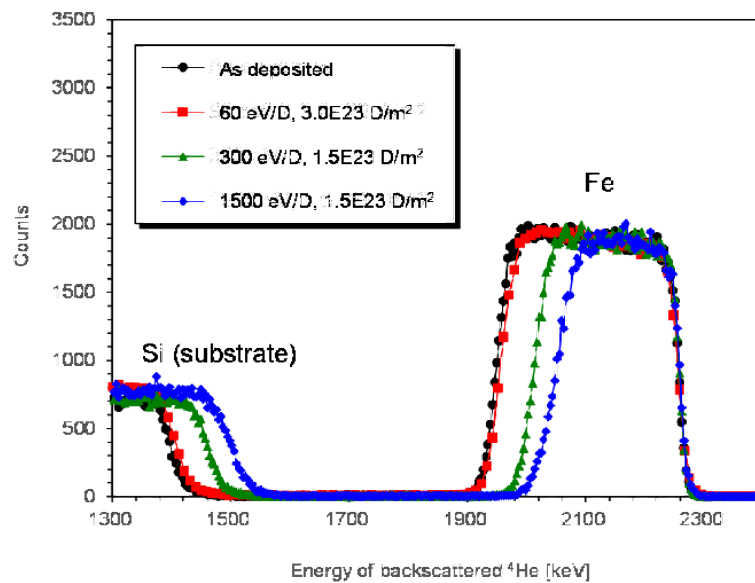Schematic view of the high-current ion source set-up.

Figure 2

RBS spectra obtained from Fe layer (on Si substrate) samples before (as deposited) and after D ion irradiation with different irradiation conditions. The primal energy of probe ^{4}He beam was 3.0 MeV. The backscattered ^{4}He was measured by a detector located at the laboratory angle of 165°.
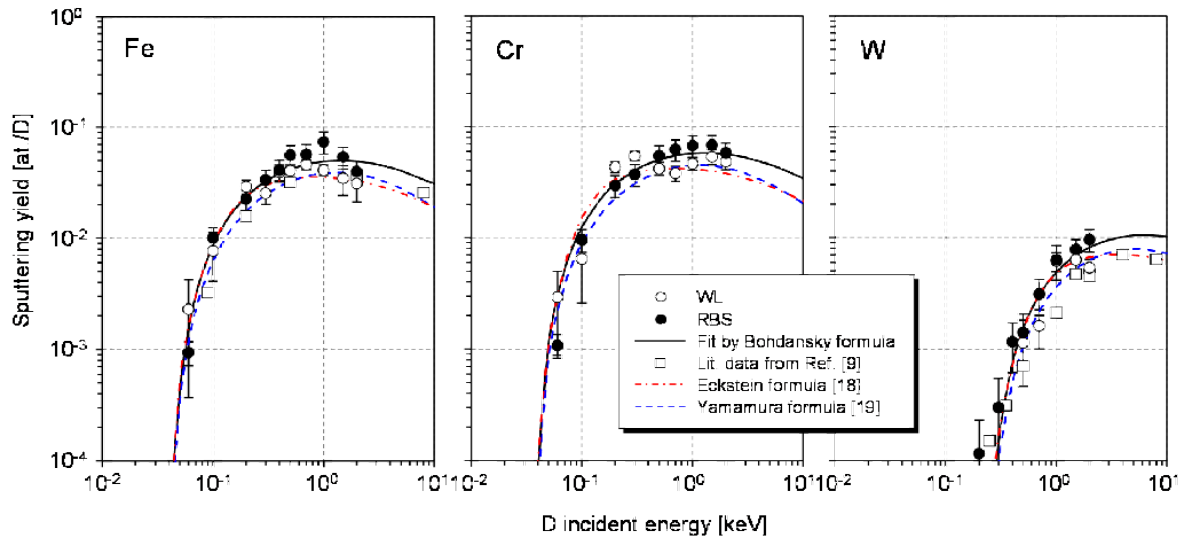
Figure 3

Experimentally determined sputtering yields of Fe, Cr and W. The solid curve is derived from the fitting by Bohdansky formula [12]. For Fe and W, literature data [9] are also shown. The dashed yield curves are from the analytical formulae by Eckstein [18] and Yamamura [19]. For the formulas see also the Appendix.
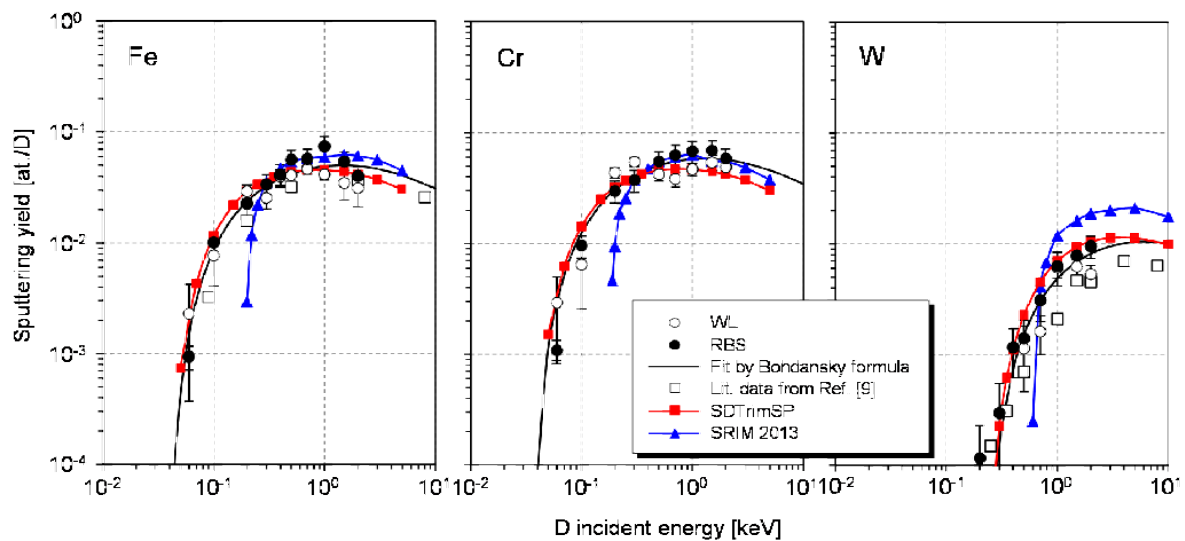

Figure 4

Comparison between experimental data obtained in this study and literature data [9], and data calculated by BCA-based simulation codes: SDTrimSP and SRIM.